JOURNAL OF SPACECRAFT AND ROCKETS
Vol. 30, No. 1, January–February 1993

Vibrational Relaxation of Anharmonic Oscillators in Expanding Flows

Stephen M. Ruffin* and Chul Park†
NASA Ames Research Center, Moffett Field, California 94035

Although the Landau-Teller vibrational model accurately predicts the vibrational excitation process in postshock and compressing flows, it underpredicts the rate of de-excitation in cooling and expanding flows. In the present paper, detailed calculations of the vibrational relaxation process of N_2 and CO in cooling flows are conducted. A coupled set of vibrational transition rate equations and quasi-one-dimensional fluid dynamic equations is solved. Multiple quantum level transition rates are computed using SSH theory. The SSH transition rate results are compared with available experimental data and other theoretical models. Vibration-vibration exchange collisions are responsible for some vibrational relaxation acceleration in situations of high vibrational temperature and low translational temperature. The present results support the relaxation mechanisms proposed by Bray and by Treanor, Rich and Rehm. Qualitative agreement with experimental results is achieved for the overall vibrational relaxation rate; however, the accuracy of the SSH results for vibration-vibration exchange transitions must be studied further and additional experimental investigations are needed for quantitative agreement.

Nomenclature

A = nozzle cross-sectional area, cm^2
E_v = energy in level v per molecule, erg
e_{vib} = vibrational energy per unit mass relative to ground state energy, erg/g
$f(\xi)$ = Keck and Carrier adiabaticity function
H = static enthalpy per unit mass, erg/g
h = Planck's constant, 6.6256×10^{27} erg-s
$K_{v,v'}$ = transition rate coefficient from v to v', cm^3/s
k = Boltzmann's constant, 1.38054×10^{-16} erg/K
$\hat{M}$ = molecular weight, g/gmole
m = mass per molecule, g
m_μ = reduced mass of the collision pair, g
N = number density, cm^3
$P_{v,v'}^{v_2 v_2'}$ = thermally averaged probability of transition from v to v' and from v_2 to v_2'
p = static pressure, dyne/cm^2
$p_{v,v'}^{v_2 v_2'}$ = velocity dependent probability of transition from v to v' and from v_2 to v_2'
Q = vector of dependent variables
q_j = dependent variable in the jth equation
R = ordinary gas constant $(\hat{R}/\hat{M}) = (k/m)$, erg/(K-g)
$\hat{R}$ = universal gas constant, 8.3143×10^7 erg/(K-gmole)
r = intermolecular distance, cm
s = steric factor
s_1, s_2 = interatomic distances, cm
T = translational temperature, K
T_{vib0} = vibrational temperature based on population at levels 0 and 1, K
t = time coordinate, s
u = streamwise flow velocity, cm/s
u_0 = precollision relative molecular velocity, cm/s
u_{0min} = minimum allowable pre-collision relative molecular velocity, cm/s
u_F = post-collision relative molecular velocity, cm/s
V = molecular interaction potential, erg
V_0 = constant in exponentially repulsive interaction potential, erg
$vmax$ = highest bound vibrational quantum level
x = streamwise spatial coordinate, cm
α = interaction range parameter in exponentially repulsive interaction potential, cm^{-1}
β_1, β_2 = constants in exponentially repulsive interaction potential
ΔE = energy transferred from translation to vibration per collision, erg
Ψ_v = vibrational wavefunction of level v, cm$^{-1/2}$
ρ = density = Nm, g/cm^3
σ_0 = effective hard sphere cross stion, cm^2
τ = vibrational relaxation time, s
Θ = collision frequency, s^{-1}
θ_v = characteristic vibrational temperature $= (E_1 - E_0)/k$, K
$\mathcal{V}_{v,v'}$ = vibrational transition matrix element for v to v' transition

Subscripts
E = thermal equilibrium condition
$jmax$ = maximum number of dependent variables
LT = Landau-Teller model
MW = Millikan and White experimental correlation
SSH = Schwartz, Slawsky and Herzfeld theory
t = stagnation condition
v = vibrational quantum level v

Superscripts
V-T = vibration-translation collisions
V-V = vibration-vibration collisions

Introduction

IN 1936, the Landau-Teller rate equation was derived to describe vibrational energy transfer in high temperature molecular gases. With vibrational relaxation times inferred from postshock flows, this equation has been shown to give

Received Feb. 6, 1992; revision received July 29, 1992; accepted for publication Aug. 3, 1992.

*Aerospace Scientist Aerothermodynamics Branch, Thermosciences Division, M.S. 230-2. Member AIAA.
†Head, Experimental Aerothermodynamics Section, Aerothermodynamics Branch, Thermosciences Division, M.S. 230-2. Associate Fellow AIAA.

or nozzle flows. These flows are characterized by a rapidly dropping translational temperature and a high degree of vibrational excitation. Related flowfields of current interest include thrust nozzles and the wakes behind high-speed vehicles such as aeroassisted space transfer vehicles and hypersonic cruise vehicles.

A number of expanding flow experiments have been conducted which attempt to quantify the increased vibrational relaxation rate in nozzles compared to postshock flows. A fairly complete table of these experiments for pure gases and gas mixtures of N_2 and CO is given by McLaren and Appleton.[1] These experiments in expanding nozzles have shown that the measured vibrational temperature is closer to the translational temperature than that predicted by the Landau-Teller model. Unfortunately, there is wide disagreement in the experimental data on the magnitude of acceleration in these flows. As discussed by Hurle,[2] some of the experimental discrepancies are due to the effect of gas impurities, shock diaphragms, and indirect vibrational temperature measurement techniques. Each of these experimental errors may enhance the overall relaxation rate. However, even the most reliable experiments indicate that for pure diatomic gases and some gas mixtures, vibrational relaxation is accelerated in expanding flows.

Theoretical models proposed by Bray[3] and by Treanor et al.[4] indicate that the faster relaxation rate may be caused by overpopulation in many of the vibrational quantum levels. This overpopulation is due to the effects of rapid vibration-vibration (V-V) exchange collisions relative to the vibration-translation (V-T) collisions. A V-T transition corresponds to a collision of molecule 1 and particle 2 in which particle 2 is either an atom or a molecule which does not happen to change its quantum state as a result of that collision. In V-V exchange collisions, one molecule gains one quantum of vibrational energy and the other loses one quantum of vibrational energy. These V-V exchanges occur with high probability because only a small amount of energy is transferred between vibration and translation. The probability of V-V collisions in which both molecules gain a quantum of vibrational energy or in which both molecules lose a quantum of energy is much less than the probability of V-T or V-V exchange collisions. The Bray model has been shown to give qualitative but not quantitative agreement with experimental data.[5] However, this model assumes a functional form for the population distributions and considers only nearest-neighbor transitions. The functional form used by Bray was proposed by Treanor et al., and neglects rapid upper level V-T transitions. The quantitative results may also be affected by use of a simple expression for the transition matrix elements rather than solving Schrödinger's equation.

In the present paper, detailed calculations of the vibrational relaxation process of pure diatomic gases in nozzle and cooling flows are conducted. N_2 and CO are studied at translational temperatures less than or equal to 4000 K. A coupled set of vibrational transition rate equations and quasi-one-dimensional fluid dynamic equations is solved. Transition rates are computed from SSH theory and multiple quantum level V-T and V-V transitions are allowed. This paper seeks to examine the collision processes responsible for accelerating vibrational relaxation in expanding flows, present computed population distributions, and investigate several aspects of SSH calculations.

Vibrational Transition Rates

SSH Formulation

SSH theory was developed to allow calculation of transition rates for molecular gases and has been shown to give reasonable predictions for nearest-neighbor V-T rates. This theory is described in detail by Schwartz, Slawsky, and Herzfeld[6] (SSH) and by Clarke and McChesney[7] and will only be outlined in this paper. SSH theory assumes end-on, colinear collisions of two rotationless particles. These assumptions introduce some error but greatly simplify the collisional analysis. The two colliding particles (molecule 1 and particle 2, say) experience an exponentially repulsive potential:

$$V = V_0 e^{-\alpha(r + \beta_1 s_1 + \beta_2 s_2)}$$

The collision partner, particle 2, can be either a molecule or an atom. The distance between the centers of mass of the two particles is given by r and the interatomic distances of particles 1 and 2 are s_1 and s_2, respectively. α, β_1, and β_2 are molecular constants which will be discussed in the next section.

Consider particles 1 and 2 initially in vibrational quantum states v and v_2, respectively, and with precollision relative velocity u_0. For each collision of these particles, the probability that they will transition to states v' and v_2', respectively, is

$$P_{v,v'}^{v_2,v_2'} = \mathcal{V}_{v,v'}^2 \, \mathcal{V}_{v_2,v_2'}^2 \frac{[(\theta_0)^2 - (\theta_F)^2]^2}{16\pi^2} \frac{\sinh(\theta_0)\sinh(\theta_F)}{[\cosh(\theta_0) - \cosh(\theta_F)]^2}$$

where

$$\theta_0 \equiv 4\pi^2 m_\mu u_0 / \alpha h$$

$$\theta_F \equiv 4\pi^2 m_\mu u_F / \alpha h$$

u_F is the postcollision relative velocity and m_μ is the reduced mass of the collision pair. The transition matrix elements are given by

$$\mathcal{V}_{v,v'} \equiv \int_{-\infty}^{\infty} \Psi_v(s_1)\, e^{-\alpha s_1} \Psi_{v'}(s_1)\, ds_1$$

where as in Sharma et al.,[8] Ψ_v and $\Psi_{v'}$ are found from numerical solutions of the one-dimensional Schrödinger equation of vibrational motion assuming an analytic Murrell-Sorbie potential. In this analysis, the vibrational levels correspond to the ground electronic state of the molecules. We can neglect dissociation and radiation because the cases presently studied are at sufficiently low temperatures. Thus, the energy lost from the translational mode must all be transferred into the vibrational mode. The energy transferred from translation to vibration is

$$\Delta E = (E_{v'} + E_{v'_2}) - (E_v + E_{v_2}) = \tfrac{1}{2} m_\mu [(u_0)^2 - (U_F)^2]$$

where E_v is the energy in vibrational state v per molecule. Integrating over all permissible initial velocities, while assuming a three-dimensional Maxwellian distribution, leads to the vibrational transition probability:

$$P_{v,v'}^{v_2,v_2'} = 2\left(\frac{m_\mu}{2kT}\right)^2 \int_{u_{0\min}}^{\infty} u_0^3 \, p_{v,v'}^{v_2,v_2'} \exp\left(-\frac{m_\mu u_0^2}{2kT}\right) du_0 \qquad (1)$$

In the present study, two different methods are investigated to determine this transition probability. Both of these methods have previously been used by other researchers and in this study a comparison of the resulting rates is given for two schemes. In the first method, the integral in Eq. (1) is computed numerically for those collisions which correspond to vibrational excitations, i.e. ΔE greater than 0. The de-excitations probabilities, i.e., those for which ΔE is less than 0, are then found by enforcing detailed balancing based on the population distribution at equilibrium:

$$P_{v_2',v'}^{v_2,v} = P_{v,v'}^{v_2',v_2} \exp\left(-\frac{\Delta E}{kT}\right) \qquad (2)$$

For exact resonance cases, i.e., $\Delta E = 0$, the probability $P_{v,v'}^{v_2,v_2'}$ is not well defined, however, in the limit as ΔE approaches 0, the resonant probability becomes

$$P_{v,v'}^{v_2,v_2'} = \mathcal{V}_{v,v'}^2 \mathcal{V}_{v_2,v_2'}^2 \left[\frac{16\pi^2 m_\mu kT}{(\alpha h)^2}\right]$$

This expression is used to compute the transition probabilities for resonant cases.

The second method of evaluating the transition probabilities utilizes an analytical expression developed by Keck and Carrier.[9] The Keck and Carrier formulation is a curve fit for the probabilities integrated over a one-dimensional Maxwellian distribution. The probabilities for vibrational excitations and resonance, i.e., ΔE greater than or equal to 0, are found via Ref. 9 and are of the form

$$P_{v,v'}^{v_2 v_2'} = \mathcal{V}_{v,v'}^2 \mathcal{V}_{v_2 v_2'}^2 \left[\frac{32\pi^2 m_\mu kT}{(\alpha h)^2}\right] \exp\left(-\frac{\Delta E}{2kT}\right) f(\xi) \qquad (3)$$

where

$$\xi \sqrt{\frac{2\pi^4 m_\mu \Delta E^2}{(\alpha h)^2 kT}}$$

The adiabaticity function $f(\xi)$ is given by

$$f(\xi) = 8\sqrt{\pi/3}\ \xi^{7/3} \exp(-3\xi^{2/3}) \qquad \text{for } \xi > 21.622$$

$$f(\xi) = \tfrac{1}{2}[3 - \exp(-2\xi/3)] \exp(-2\xi 3) \qquad \text{for } 0 \le \xi \le 21.622$$

The de-excitation probabilities are again found from detailed balancing as shown in Eq. (2). Use of the Keck and Carrier expression is much faster than the numerical integration method and a comparison of the two methods is presented in subsequent figures.

We can now compute the transition rate coefficient $K_{v,v'}$, which can be thought of as the fraction of molecules in state v that transition to state v' per unit time per unit number density. The transition rate coefficient for molecule 1 is found by summing over all possible transitions of particle 2:

$$K_{v,v'} = \frac{\Theta}{N^2} \sum_{v_2=0}^{vmax2} \sum_{v_2'=0}^{vmax2} N_{v_2} P_{v,v'}^{v_2 v_2'}$$

where N_{v_2} is the number of particles 2 in state v_2 per unit volume and N is the total number density (i.e., total number of particles per unit volume). The collision frequency (number of collisions of particles 1 and 2 per unit time per particle) is

$$\Theta = s\, N\, \sigma_0 \sqrt{8\pi kT/m_\mu}$$

where σ_0 is the effective hard sphere cross section. s is a steric factor which takes into account the fact that most collisions are not colinear. The theoretical value of $s = 1/9$ for diatomic collision partners is used for the present computations. The definition of this steric factor is given in Refs. 7 and 10. There are several sources of error in the computed transition rates. The chief sources of error include the SSH assumptions of colinear collisions and an exponentially repulsive interaction potential, and uncertainties in molecular constants such as σ_0. Because of these errors and uncertainties, the transition rates must be adjusted to match experimental data. In this study, the computed ground state transition rate coefficient for V-T transitions is adjusted to match the value inferred from shock tube data compiled by Millikan and White.[11] In shock-tube experiments, the Landau-Teller equation is used with good success to predict the postshock vibrational relaxation. The equilibrium ground state transition rate can be inferred from the Millikan and White vibrational relaxation time by using

$$K_{1,0E}^{VT} = [N\, \tau_{MW}(1 - e^{-\theta_v/T}]^{-1}$$

The hard sphere cross section σ_0 appears only as a multiplier in the transition rate expression and can be used to adjust the computed rates to match known experimental rates. In the present study, σ_0 is chosen so that the computed equilibrium ground state transition rate matches the Millikan and White value. The value of σ_0 thus obtained is used for all of the V-T and V-V transition rates and is generally within an order of magnitude of tabulated values in texts such as Ref. 12. A similar correction procedure has previously been used by Sharma et. al.[8] and also by Landrum and Candler[13] in vibrational transition rate calculations. The relationship of all other rates to the ground state rate is obtained from the SSH formulation using the molecular constants described in the next section.

Molecular Constants

Computing the transition rates using SSH theory requires specification of the molecular constants α, β_1, and β_2. The transition rates are strongly dependent on the value of the interaction range parameter α, and are much weaker functions of β_1 and α_2. The α primarily defines the slope of the interaction potential as a function of distance between particles 1 and 2. β_1 and β_2 define the change in potential as functions of the interatomic distances of the two particles. Approximate values for β_1 and β_2 can be found by considering purely end-on collisions in which only the nearest two atoms of particles 1 and 2 contribute to the interaction potential. For homonuclear molecules such as N_2, $\beta_1 = \beta_2 = -0.5$. This value is used in all of the present calculations.

The value of α has been a source of debate and uncertainty for years. As pointed out by Billing and Fisher,[14] molecular beam data gives α in the range 3-4 A^{-1} for N_2. Radzig and Smirnov[15] quote an experimental value of $\alpha = 3.16A^{-1}$ for N_2 and $\alpha = 3.47\ A^{-1}$ for CO. However in performing calculations of N_2 transition rates using a semiclassical model, Billings and Fisher[14] find that $\sigma = 4.0\ A^{-1}$ gives better agreement with V-T transition rate data than $\alpha = 3.16\ A^{-1}$. In the original SSH paper, Schwartz et al.[6] determined α by fitting the exponentially repulsive potential to the Lennard-Jones potential. This gives $\alpha = 4.72\ A^{-1}$ for N_2 and $\alpha = 4.87\ A^{-1}$ for CO. Sharma et al.[8] used a value of $\alpha = 1.0A^{-1}$ for N_2 and predicted a severe bottleneck in the transition rates. Through discussion with the authors of that reference it was revealed that $\alpha = 1.0\ A^{-1}$ was used because at some given temperature and given effective cross section σ_0, the computed ground state transition rate required little adjustment to match the ground state transition rate inferred from the experimental data of Millikan and White. Finally, Landrum and Candler[13] obtained a very high value of α but have since recognized[16] that this a was obtained by incorrectly matching the interatomic Murrell-Sorbie potential to the intermolecular potential. The molecular beam results and the values obtained by matching the Lennard-Jones potential provide the most plausible range of α for N_2 and CO.

Since one of our goals is to accurately predict transition rates, the best value of α to use in SSH calculations is one which allows computed SSH rates to match experimentally observed properties. Ideally, we would like the SSH rates to match the true ground state magnitude at a specific temperature, ground state temperature dependence, and the scaling of the other levels relative to the ground state rate.

There is a vast difference in the amount of experimental data available for V-T and V-V rates. The Millikan and White data provides a wealth of information on the ground state magnitude and temperature dependence for the V-T rates. Experimental data on the scaling of other V-T levels is sparse but calculated results of this scaling based on a semiclassical model[14] provides additional data with which to compare. Thus, in the present study, the ground state magnitude and temperature dependence of the V-T rates will be matched to experimental data. The scaling of all other V-T rates to the ground state rate will be compared to a semiclassical model. This matching procedure is described further in the following paragraphs.

In this study, we match the magnitude of the ground state V-T rate at a reference temperature by choosing the appropriate value of σ_0 as described in the previous section. The ground

state temperature dependence and the scaling of the upper levels are strongly influenced by the value of α. Because SSH uses only a short range potential, it is possible that the value of α chosen to match V-V exchange rate data may be somewhat different than the α which matches V-T data. Thus we will define an $\alpha_{V\text{-}T}$ to be used in computing V-T rates and an $\alpha_{V\text{-}V}$ for V-V rates.

As shown by Landrum and Candler,[13] α has significant effect on the scaling of the other levels relative to the ground state rate. However, α also has a strong effect on temperature dependence of the ground state V-T probabilities. We can show from Eq. (3) that the dominant temperature dependence of the ground state rates is in the exponential term:

$$P_{1,0}^{0,0} \sim \exp\left[-\left(\frac{m_\mu k \theta_v^2}{(\alpha h)^2 T}\right)^{1/3} \right]$$

The constants h, k, m_μ, and θ_v are known with much greater certainty than α, so we can also write

$$P_{1,0}^{0,0} \sim \exp(-T^{1/3}\,\alpha^{-2/3}) \tag{4}$$

Since the Millikan and White correlation gives the ground state rate as a function of temperature, we can determine $\alpha_{V\text{-}T}$ by finding the value which gives the same temperature dependence as the experimental data.

According to Landau-Teller Theory, the V-T transition rates are independent of the population distributions because $P_{1,0}^{0,0} \approx P_{1,0}^{1,1} \approx P_{1,0}^{2,2} \approx \ldots$ Thus the ground state probability is found from

$$\frac{\Theta}{N} P_{1,0(\text{MW-LT})}^{0,0} = [N\,\tau_{MW}\,(1 - e^{-\theta_v/T})]^{-1}$$

with the aid of Millikan and White data. The SSH probabilities are found by two methods: numerically integrating over a three-dimensional velocity distribution via Eq. (1) or by using the Keck and Carrier expression, Eq. (3). Figure 1 shows the V-T transition probabilities for N_2 at $p = 1$ atm inferred from Millikan and White data and from the computed ground state probabilities. For this plot, σ_0 is chosen so that the SSH rates agree with Millikan and White at $T = 8000$ K. Note that there is little difference between the results when numerically integrating the three-dimensional velocity distribution and when using the Keck and Carrier formulation. As expected, each of these methods gives rates which have the temperature dependence shown in Eq. (4) over most of the temperature range shown. The Radzig and Smirnov value of $\alpha_{V\text{-}T} = 3.16\ A^{-1}$ and the Schwartz et al. value of $\alpha_{V\text{-}T} = 4.72\ A^{-1}$ do not quite match the Millikan and White slope. For N_2, $\alpha_{V\text{-}T} = 3.90\ A^{-1}$ was found to allow the SSH results to agree with the experimentally observed temperature dependence and this value is used for the present N_2 calculations.

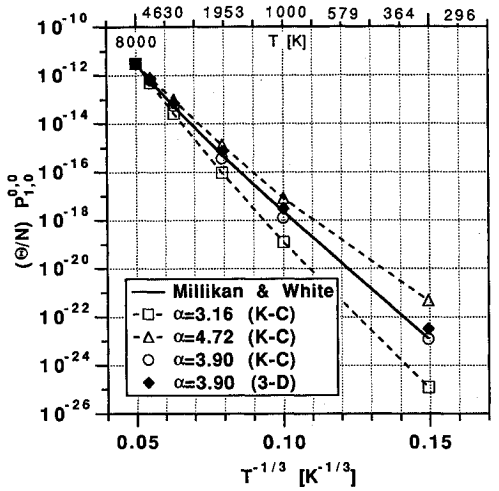

Fig. 1 Comparison of computed ground state V-T transition probabilities from SSH theory to Millikan and White data for N_2 at p = 1 atm.

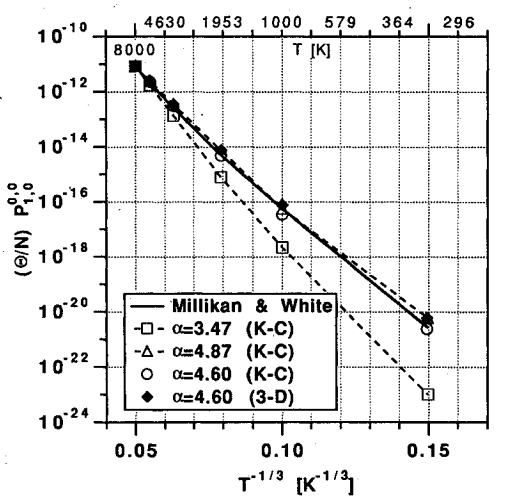

Fig. 2 Comparison of computed ground state V-T transition probabilities from SSH theory to Millikan and White data for CO at p = 1 atm.

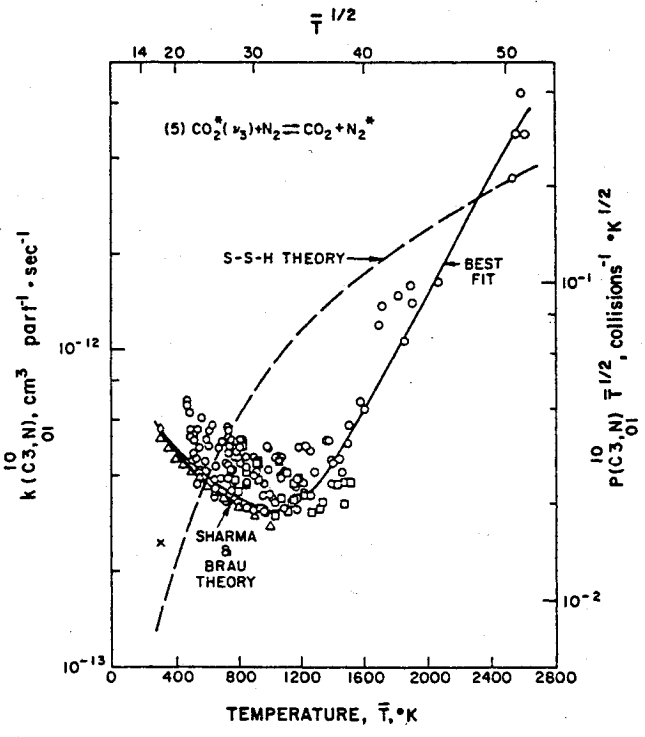

Fig. 3 Comparison of SSH results to experimental results for near-resonant CO_2-N_2 mixtures. This figure is reprinted from Taylor and Bitterman.[17] See Ref. 17 for the sources of experimental data points.

Figure 2 shows similar ground state rates for the CO molecule at $p = 1$ atm. The SSH results using $\alpha_{V\text{-}T} = 4.87\ A^{-1}$ agree fairly well with the Millikan and White temperature dependence. However, it is found that $\alpha_{V\text{-}T} = 4.60\ A^{-1}$ gives the best agreement with data and thus is used for the present calculations involving CO. Once again the Keck and Carrier formulation and the numerical integration method give nearly the same temperature dependence.

Now, we would also like to perform a similar correction procedure for V-V exchange rates. However, there is practically no experimental data on the V-V exchange rates of N_2 and CO at temperatures of interest in this paper. Thus, it is

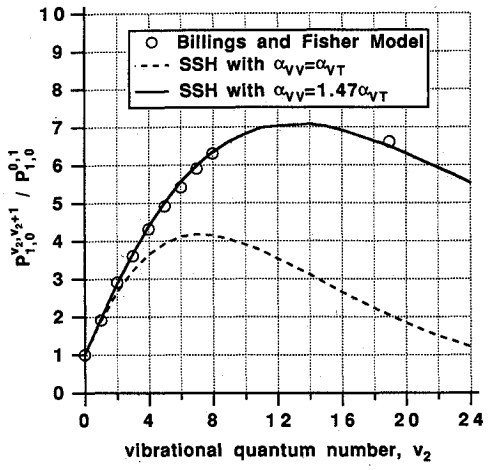

Fig. 4 Comparison of computed V-V probabilities for Nsdo4(2) using SSH theory and the Billings and Fisher semiclassical model at $T = 2000$ K with $\alpha_{V\text{-}T} = 4.0$ A^{-1}.

difficult to independently verify the accuracy of the ground state V-V exchange rates and the scaling of all other V-V exchange rates relative to the ground state rate. Virtually all of the V-V exchange transition rate data for N_2 and CO is measured in laser systems at temperatures below 1000 K or in CO_2-N_2 gas mixtures at T below 2600 K. A comparison of SSH results to measured V-V exchange rates in CO_2-N_2 mixtures is given by Taylor and Bitterman[17] and is reprinted in Fig. 3. The near resonant V-V exchange rate is shown as a function of temperature. The SSH rates fail to accurately match the magnitude and temperature dependence of the measured V-V rates especially at very low temperatures. The SSH rates are in error within a factor of 50. Sharma and Brau[18] indicate that for near resonant V-V exchange rates and/or at low temperatures, long-range molecular interaction forces which are not included in SSH theory become important. SSH theory uses an exponentially repulsive potential which only takes into account short-range effects. Because of uncertainties in the V-V exchange rates, the effects of these transitions will be studied by using SSH rates and by performing a parametric study involving various V-V exchange rates and various values of $\alpha_{V\text{-}V}$. In the parametric study, all V-V exchange rates are multiplied by various constant factors to study the effect of changes in the magnitude of these rates. The effect of the scaling of all V-V exchange rates relative to the ground state is investigated by using different values of $\alpha_{V\text{-}V}$.

An approximate value of $\alpha_{V\text{-}V}$ is determined by comparing SSH computed V-V exchange rates to published results from the Billing and Fisher semiclassical model. The three-dimensional Billing and Fisher transition rate model uses an interaction potential which includes both short-range and long-range forces. Thus, this model is more realistic than SSH theory. Figure 4 shows the V-V exchange probabilities for N_2 relative to the ground state rate at $T = 2000$ K. The V-V exchange probability initially increases and then decreases with quantum number. The increase is due to the increase in matrix elements with quantum number. The rates then decrease for the upper levels because anharmonic resonance defect increases for these rates. For example, because of anharmonicity, the energy transferred from vibration to translation in the $P^{24,23}_{1,0}$ transition is greater than the energy transferred in the $P^{4,3}_{1,0}$ collision. Because the energy transferred is greater in the upper level transition, the V-V exchange probability is lower in these upper levels. The combined effects of increasing matrix elements and increasing resonance defect produce a maximum in the V-V exchange probabilities shown. The SSH results using $\alpha_{V\text{-}V} = \alpha_{V\text{-}T} = 4.0\ A^{-1}$ do not agree with the more complete Billing and Fisher model. It is found that for $T = 2000$ K, using $\alpha_{V\text{-}V} = 1.47\alpha_{V\text{-}T}$ for the SSH rates provides very good agreement with the semiclassical results. Clearly, either a model more accurate than SSH must be used for V-V rates or similar comparisons must be performed at a variety of temperatures in order to validate any choice of $\alpha_{V\text{-}V}$. Both of these efforts are the subject of future work. In this paper, the effect of using various values of $\alpha_{V\text{-}V}$ is studied.

SSH Results

The vibrational transition rates are functions of the translational temperature and the population distribution and thus vary in a gas in thermal nonequilibrium. Some general features of the transition rates can be examined by observing the nearest-neighbor rates, $K_{v,v+1}$, for a Boltzmann distribution.

Figure 5 shows the nearest-neighbor V-T transition rates for N_2 at $T = 2000$ K. The vibrational levels are populated according to a Boltzmann distribution at $T_{vib} = 4000$ K. SSH rates for various values of $\alpha_{V\text{-}T}$ and the rates assumed by Landau-Teller theory are shown. In each of the cases, the transition rates increase with quantum number because of increasing transition matrix elements. The SSH rates at the lower levels are near the Landau-Teller rates. The upper level SSH rates are higher than the Landau-Teller rates because anharmonicity increases the probabilities of these closely spaced levels relative to the harmonic oscillator Landau-Teller model. The lower values of α are found to give somewhat faster rates than the higher values of α. The SSH rates for $\alpha_{V\text{-}T} = 3.9\ A^{-1}$ are

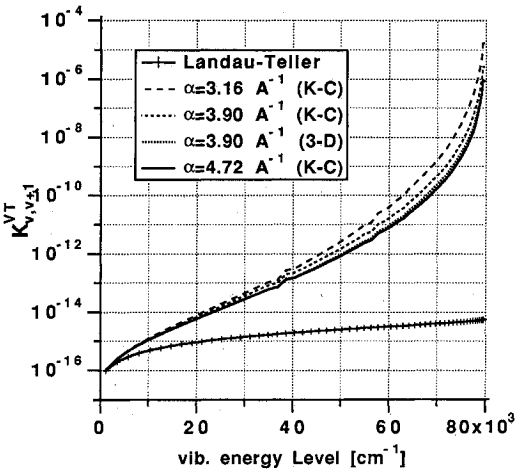

Fig. 5 Computed V-T transition rates for N_2 using SSH theory and various values of α. $T = 2000$ K and vibrational levels populated in a Boltzmann distribution at $T_{vib} = 4000$ K.

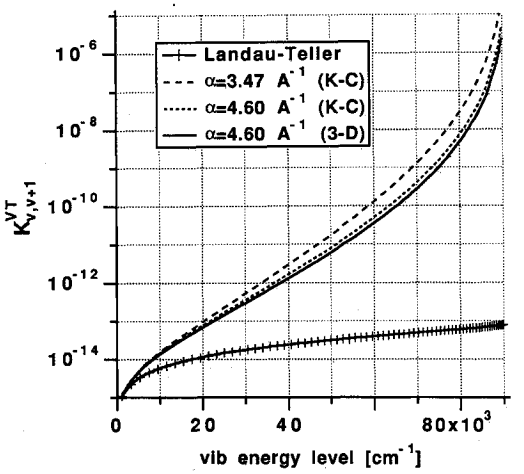

Fig. 6 Computed V-T transition rates for CO using SSH theory and various values of α. $T = 2000$ K and vibrational levels populated in a Boltzmann distribution at $T_{vib} = 4000$ K.

shown using the Keck and Carrier expression and the three-dimensional numerical formulation. There is little difference in the results of these two methods.

Figure 6 shows the nearest-neighbor V-T rates for CO at the same conditions. As in the N_2 case, the SSH rates are higher than those assumed by the Landau-Teller model. Once again, it is found that the Keck and Carrier expression and the three-dimensional formulation give very similar results. Because the Keck and Carrier formulation requires much less CPU time, it is used in all of the present computations of the vibrational relaxation process.

Nozzle Flow Formulation

Calculation of all of the transition probabilities and rates for one temperature is computationally expensive. In a general two-dimensional or three-dimensional flow, we would need to compute these for every temperature in the flowfield and solve a vibrational rate equation for each vibrational level, and solve fluid dynamic equations simultaneously. Nitrogen has 57 bound quantum states so we would need to solve over 60 coupled equations for each grid node. Furthermore, if a time marching scheme is used, the CPU requirement would be much greater. Thus, detailed calculations of the vibrational transition rate equations in general two-dimensional or three-dimensional flows are prohibitively expensive.

Fortunately, vibrational relaxation in expanding flows has been studied experimentally in geometrically simple nozzles. In many of these experiments the nozzle area increases slowly and in the present calculations we make the quasi-one-dimensional approximation. This approximation greatly reduces the CPU requirement relative to two-dimensional and three-dimensional calculations because the number of grid nodes and equations are reduced. The flows studied are also assumed to be in steady state and inviscid.

Vibrational Rate Equations

The vibrational transition rate master equations are of the form:

$$\frac{\mathrm{D}(N_v/\rho)}{\mathrm{D}t} = \left(\frac{N}{\rho}\right) \sum_{v'=0}^{vmax} (K_{v',v} N_{v'} - K_{v,v'} \mathrm{N}_v)$$

where N_v is the number of molecules 1 in state v per unit volume. We can then use fluid transport relations to convert the material derivative to finite volume form and write the quasi-two-dimensional, steady, vibrational transition rate equation as

$$\frac{\partial N_V}{\partial x} = \left(\frac{N}{u}\right) \sum_{v'=0}^{vmax} (K_{v',v} N_{v'} - K_{v,v'} N_v) - \frac{N_v}{A}\frac{\mathrm{d}A}{\mathrm{d}x} - \frac{N_v}{2u^2}\frac{\partial(u^2)}{\partial x}$$

The vibrational energy per unit mass is

$$\mathrm{e}_{\mathrm{vib}} = \frac{1}{\rho} \sum_{v=0}^{vmax} E_v N_v \tag{5}$$

In the present calculations, E_v and thus e_{vib} are measured relative to their ground state (i.e., $v = 0$) values. By differentiating this equation and substituting in the previous equation we can show that the quasi-one-dimensional, steady, vibrational energy rate equation is

$$\frac{\mathrm{e}_{\mathrm{vib}}}{\partial x} = \frac{1}{u}\frac{R}{k} \sum_{v=0}^{vmax} \sum_{v'=0}^{vmax} E_v (K_{v',v} N_{v'} - K_{v,v'} N_v) \tag{6}$$

where k is Boltzmann's constant and $R = (\hat{R}/\hat{M})$ is the ordinary gas constant.

Although we employed the quasi-one-dimensional approximation, if typical time marching numerical schemes are used to solve the finite difference form of the governing equations the calculations would still be computationally very expensive. However, the steady, quasi-one-dimensional differential equations are parabolic and involve only one independent variable. Thus, we can take advantage of the quasi-one-dimensional formulation by performing one spatial march rather than iterating in time. For this study, an efficient, implicit, space marching, solver called STIFF7 is utilized. STIFF7 numerically computes Jacobians and integrates a coupled set of quasilinear, partial differential equations and is described in more detail by Lomax.[19] An equation is termed quasilinear if the highest-order derivatives appear explicitly and to the first power only. If Q is a set of dependent variables,

$$Q \equiv \begin{pmatrix} q_1 \\ q_2 \\ \cdot \\ \cdot \\ \cdot \\ q_{jmax} \end{pmatrix}$$

then STIFF7 solves a coupled set of partial differential equations each of the form

$$\frac{\partial q_i}{\partial x} = f\left(q_1, q_2, \ldots, q_{jmax}, \frac{\partial q_1}{\partial x}, \frac{\partial q_2}{\partial x}, \ldots, \frac{\partial q_{jmax}}{\partial x}, x\right)$$

x is the independent variable taken as the streamwise coordinate in the present calculations. If we take u^2 and N_v as dependent variables, then the vibrational transition rate and energy rate equations shown above fit the form required for the solver. We may now develop an equation for u^2 by starting from the fluid dynamic equations for steady, quasi-one-dimensional, inviscid flow:

$$\rho u A = \text{const}$$

$$\rho u \frac{\partial u}{\partial x} = -\frac{\partial p}{\partial x}$$

$$H + u^2/2 = H_t = \text{const}$$

Assuming translational/rotational equilibrium and considering only flows with no chemical reactions gives

$$H = 7/2RT + e_{\mathrm{vib}}$$

We have also used the equation of state for a thermally perfect gas, $p = \rho RT$, which can be obtained from kinetic theory. Differentiating and combining each of the previous equations yields the required equation for u^2 which describes the fluid dynamics of the flow:

$$\frac{\partial(u^2)}{\partial x} = \frac{(2/\mathrm{A})(\mathrm{d}A/\mathrm{d}x)(H_t - e_{\mathrm{vib}} - 1/2u^2) + 2(\partial e_{\mathrm{vib}}/\partial x)}{\{3 - [(H_t - e_{\mathrm{vib}})/u^2]\}}$$

Thus, for the detailed calculation of vibrational populations coupled to fluid equations, the set of dependent variables is

$$Q = \begin{pmatrix} u_2 \\ N_1 \\ N_2 \\ \cdot \\ \cdot \\ \cdot \\ N_{vmax} \end{pmatrix}$$

In this formulation, e_{vib} and its derivative are found from Eqs. (5) and (6), respectively.

In converging-diverging nozzle simulations, a numerical difficulty arises because the mass flow rate for thermal nonequilibrium flow is not known a priori. If the mass flow rate

chosen is too high, then a shock will begin to form upstream of the nozzle throat and subsonic flow will exist on both sides of the throat. If the mass flow rate chosen is too low, then subsonic flow will also exist on each side of the throat. A good discussion of this critical mass flow problem and various solutions are given by Hall and Treanor.[20] In the present calculations, an automated trial-and-error method is used with the initial guess guided by the equilibrium and frozen limits. This method is automated by checking the pressure and Mach number at each step. If at a given step the pressure is 2% greater than at the previous step, then a compression wave is forming and the calculation is restarted at a slightly lower Mach number but with the same total pressure and temperature. For locations downstream of the throat, if the Mach number is < 1 when $A/A^* > 1.2$, then the computation is restarted at a higher Mach number with the same total conditions. Unlike other methods, such as perturbation methods, the present scheme preserves the exact nozzle geometry and is simple to implement.

Landau-Teller Model

We can also use the STIFF7 solver to investigate the performance of the Landau-Teller equation. This is done by omitting the population distribution equations and instead of using the true energy rate equation we use the Landau-Teller relaxation equation. For a Landau-Teller solution, we have

$$Q = \begin{pmatrix} u^2 \\ e_{\text{vib}} \end{pmatrix}$$

where

$$\frac{\partial e_{\text{vib}}}{\partial x} = (1/u)\frac{(e_{\text{vib}E} - e_{\text{vib}})}{\tau_{\text{LT}}}$$

and τ_{LT} is the vibrational relaxation time. In this study, τ_{LT} is obtained from Millikan and White experimental data. The equilibrium vibrational energy per unit mass for a harmonic oscillator is

$$e_{\text{vib}E} = \frac{R\theta_v}{e^{\theta v/T} - 1}$$

Isothermal Cooling Simulation

Relaxation of a vibrationally excited gas to equilibrium at a lower, constant translational temperature is studied. This simulation is analogous to the vibrational nonequilibrium process in an expanding flow and illustrates many of the same features. This simulation is easier to conduct than the nozzle flow calculations because no critical throat mass flow rate must be determined for the present isothermal, constant-volume case.

The same solver is also used to compute vibrational relaxation of a constant volume of gas at constant translational temperature. Such simulations allow study of many aspects of vibrational relaxation without additional fluid dynamic complexities. Isothermal simulations are conducted by adding the following constraints to the relations described in the previous sections: $T = \text{const}$, $dT/dx = 0$, $A = \text{const}$, $dA/dx = 0$, $u = 1$, and $du/dx = 0$. With the velocity fixed at unity, the variable x becomes the time coordinate.

Considerable computational time can be saved if some very improbable multiple-quantum transitions are neglected. Transition rate calculations for N_2 and CO at $T < 4000$ K reveal very small probabilities for collisions in which jumps of greater than two quantum levels are achieved. Thus in the present isothermal cooling simulation, all 57 bound levels of N_2 are computed and only collisional jumps of up to four quantum levels are considered. The required CPU time for each of these simulations is approximately 25 min on a Cray YMP.

Initially, a volume of N_2 at $p = 1$ atm is assumed to be at an equilibrium Boltzmann distribution at $T_{\text{vib}} = 4000$ K. Then at

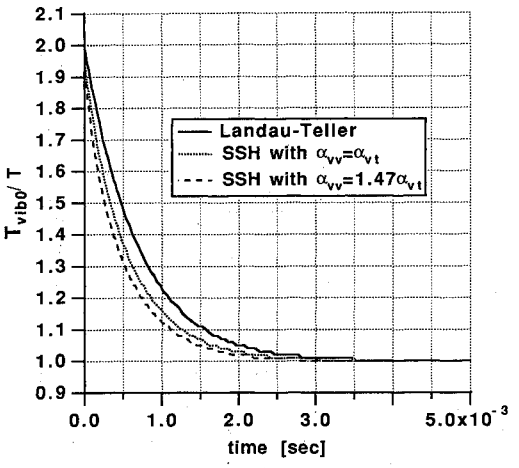

Fig. 7 Ground state vibrational temperature vs time for N_2 cooling simulation with $\alpha_{V\text{-}T} = 3.9$ A^{-1}, $T = 2000$ K, and initial $T_{\text{vib}} = 4000$K.

$t \geq 0$, the translational temperature is fixed at $T = 2000$ K and the gas is allowed to vibrationally relax. Figure 7 shows the time history of the ground state vibrational temperature for the Landau-Teller model and the SSH formulation with 57 bound vibrational levels and with $\alpha_{V\text{-}T} = 3.9\,A^{-1}$. The ground state vibrational temperature characterizes the population distribution in the lowest levels and is found from

$$\frac{N_1}{N_0} = \exp\left[-\frac{E_1 - E_0}{kT_{\text{vib}0}}\right]$$

SSH results are shown with $\alpha_{V\text{-}V} = \alpha_{V\text{-}T}$ and with $\alpha_{V\text{-}V} = 1.47\alpha_{V\text{-}T}$. We see that each of the SSH cases shows faster relaxation than Landau-Teller model in this cooling case. The higher value of $\alpha_{V\text{-}V}$ results in faster relaxation than the lower value.

The evolution of the computed population distributions for these two cases are shown on Figs. 8 and 9. These plots show the number density normalized by the equilibrium number density so that constant-slope line implies a Boltzmann distribution and a zero-slope line at unity denotes equilibrium distribution at the translational temperature. The overall impression of these results is that over almost the entire relaxation process, the lower levels distributions are not far from Boltzmann at some vibrational temperature and the uppermost levels are in equilibrium at T. The upper levels reach equilibrium very quickly because of the very rapid V-T transitions for these levels. Closer inspection of the lower and middle levels reveals that slope increases with quantum number which implies that overpopulation exists for these levels. This overpopulation is due to V-V exchange transitions and is more extreme when $T_{\text{vib}} \gg T$, i.e., near the beginning of this cooling process. This overpopulation would have been much more severe if the initial vibrational temperature were much higher than the translational temperature. Even the relatively mild overpopulation for the temperatures shown is sufficient to accelerate the overall vibrational relaxation. The use of $\alpha_{V\text{-}V} = 1.47\alpha_{V\text{-}T}$ vs the lower value of $\alpha_{V\text{-}V}$ increases the effect of the V-V exchange transitions, thus further accelerating vibrational relaxation and delaying the onset of the uppermost level equilibrium caused by V-T transitions.

Parametric Study

Because there is uncertainty in the SSH rates for V-V exchange transitions, a parametric study was conducted involving various values of V-V exchange rates and $\alpha_{V\text{-}V}$. The cooling simulation was re-computed using V-V exchange rates that are all multiplied by a factor of 0.001, 0.01, 0.1, 1, 10, 100,

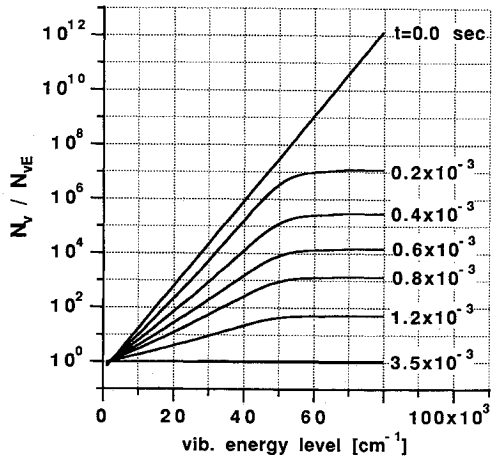

Fig. 8 Normalized population distribution for Nsdo4(2) cooling simulation with $\alpha_{V\text{-}T} = 3.9\ A^{-1}$ and $\alpha_{V\text{-}V} = \alpha_{V\text{-}T}$. Vibrational population is normalized by the equilibrium distribution.

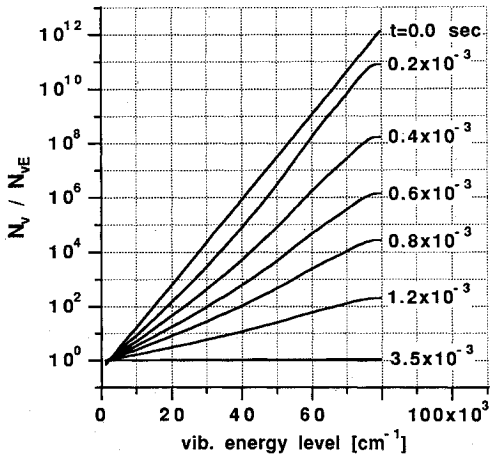

Fig. 9 Normalized population distribution for Nsdo4(2) cooling simulation with $\alpha_{V\text{-}T} = 3.9\ A^{-1}$ and $\alpha_{V\text{-}V} = 1.47\alpha_{V\text{-}T}$. Vibrational population is normalized by the equilibrium distribution.

and 1000. In addition, the following values of $\alpha_{V\text{-}V}$ were studied: $\alpha_{V\text{-}V} = \alpha_{V\text{-}T}$, $\alpha_{V\text{-}V} = 1.47\alpha_{V\text{-}T}$, $\alpha_{V\text{-}V} = 2.0\alpha_{V\text{-}T}$, and $\alpha_{V\text{-}V} = 2.5\alpha_{V\text{-}T}$. Figure 10 gives the ratio of the Landau-Teller relaxation time to the overall relaxation time found from the full master equation solver. The overall relaxation time in this figure is defined as the time required for $(e_{vib} - e_{vibE})$ to fall to $1/e$ of its initial value. Figure 10 shows that with both $\alpha_{V\text{-}V} = \alpha_{V\text{-}T}$ and $\alpha_{V\text{-}V} = 1.47\alpha_{V\text{-}T}$ the overall relaxation rate is approximately 1.4 times faster than the rate assumed by the Landau-Teller model. We also see that for these two values of $\alpha_{V\text{-}V}$, the overall relaxation time remains practically constant even when multiplying or dividing by factors of 1000. This observation can be explained by considering the relaxation models proposed by Bray[3] and by Treanor et al.[4] These models indicate that even without multiplying the V-V exchange rates by large factors, at the temperatures studied in this paper the V-V exchange rates are already much faster than the V-T rates in the lower vibrational levels. The vibrational population quickly attains a quasi-equilibrium distribution in a time much shorter than the overall relaxation time. For flows in which $T_{vib} > T$ this results in an overpopulation. Multiplying all of the V-V exchange rates by ten, for example, causes the quasi-equilibrium to be reached ten times faster, but compared to τ_{LT} this distribution is already achieved instantaneously. As long as the V-V exchange ground state probability is much greater than the V-T rate (as it is for moderate and low temperatures), its exact value has little effect on the overall vibrational relaxation rate. This observation suggests that even if SSH theory significantly underpredicts the true magnitude of the V-V exchange rates, the overall relaxation rate does not change very much for these types of flows.

Multiplying all of the V-V exchange rates by a constant factor greater than unity has little effect on the overall relaxation rate but, as shown in Fig. 10, different values of $\alpha_{V\text{-}V}$ do affect the overall rate. The scaling of the V-V exchange probabilities relative to the ground state rate influences the population distribution and overall relaxation rate. As shown in Figs. 8 and 9, the higher values of $\alpha_{V\text{-}V}$ increase the level of overpopulation in the middle and upper levels. However, Fig. 10 demonstrates that only values of $\alpha_{V\text{-}V}$ greater than or equal to 2.0 $\alpha_{V\text{-}T}$ give a significantly faster overall relaxation rate. Nozzle flow experiments of N_2 and CO at temperatures from 2000 K to 4000 K observe overall relaxation rates which are 3–100 times faster than the Landau-Teller value. If there are small or moderate errors in the scaling of the V-V exchange rates computed from SSH theory then the overall relaxation rate is less than two times faster than the Landau-Teller value for the case considered. Only very significant modifications to the V-V exchange rates computed from SSH theory result in overall relaxation rates much faster than two for this case.

Nozzle Flow Results

A number of expanding flow experiments have been conducted which quantify the faster vibrational relaxation rate in nozzles compared to postshock flows. The test case chosen in this study was performed by von Rosenberg et al.[21] and measures vibrational relaxation of pure CO in a two-dimensional nozzle. A schematic of the nozzle is shown in Fig. 11. In the experiment a shock is reflected off the end wall upstream of the nozzle. The shock reflection forms a reservoir of high-temperature, high-pressure gas which expands through the nozzle. This case was chosen because its results are representative of those experiments which had little uncertainty due to impurities, shock diaphragms, and indirect vibrational temperature

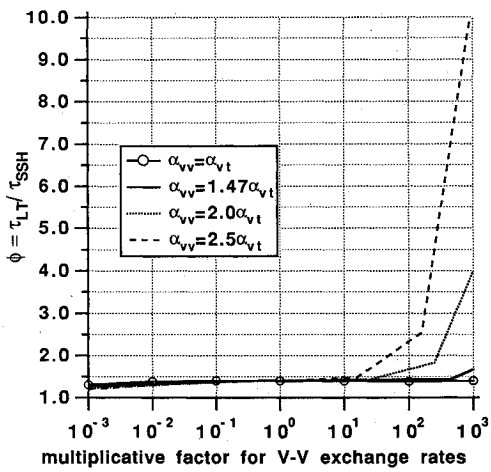

Fig. 10 Overall relaxation time for the cooling simulation using various values of $\alpha_{V\text{-}V}$ and various multiplicative factors for the V-V exchange rates.

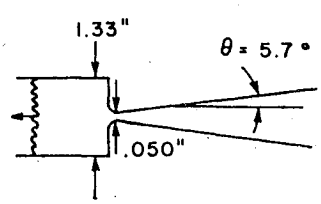

Fig. 11 Schematic of von Rosenberg et al. two-dimensional nozzle geometry.

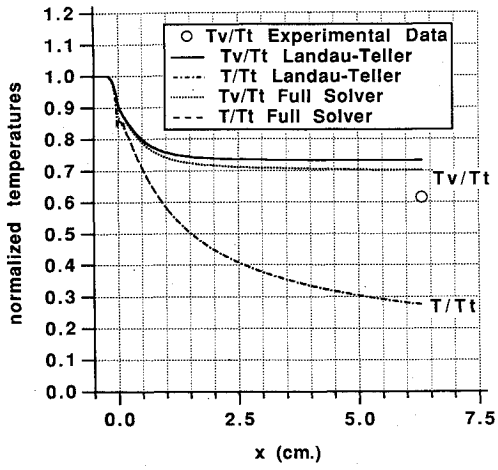

Fig. 12 Computed and experimental ground state vibrational temperature along the von Rosenberg et al.[21] nozzle. $T_t = 4000$ K, $p_t = 14.8$ atm, $\alpha_{V\text{-}T} = 4.6\ A^{-1}$ and $\alpha_{V\text{-}V} = 1.47\alpha_{V\text{-}T}$.

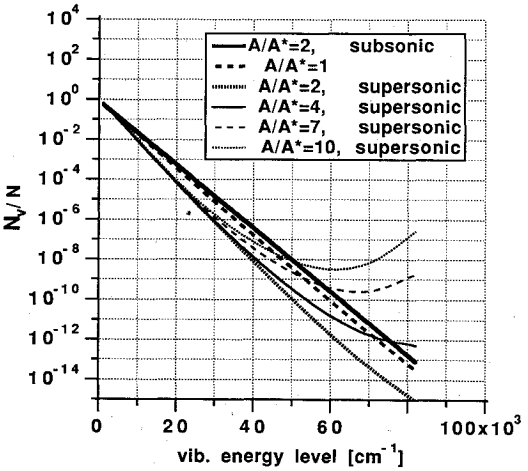

Fig. 13 Computed normalized population distribution for von Rosenberg et al.[21] nozzle flow. $T_t = 4000$ K, $p_t = 14.8$ atm, $\alpha_{V\text{-}T} = 4.6\ A^{-1}$ and $\alpha_{V\text{-}V} = 1.47\alpha_{V\text{-}T}$.

measurement techniques. The von Rosenberg et al.[21] experiment uses an infrared emission technique to measure the vibrational temperature characterizing the population distribution in the lowest levels. The vibrational temperature is measured in a nozzle at an area ratio of $A/A^* = 10$ for various total temperatures and total pressures. The full solver is computationally intensive because probabilities and transition rates must be computed at each step and because several tries are needed to determine the critical throat mass flow rate. Because of limited CPU resources, the full calculation is performed for only the first 57 bound levels of CO. Collisional jumps of up to two quantum levels are considered for this computation. Once the critical mass flow rate is determined, the nozzle flow calculation requires approximately 90 min of CPU time on a Cray YMP.

Computed and experimental results for $T_t = 4000$ K and $p_t = 14.8$ atm are shown in Figs. 12 and 13. For the SSH results, the ground state vibrational temperature is shown using $\alpha_{V\text{-}T} = 4.6\ A^{-1}$ and $\alpha_{V\text{-}V} = 1.47\alpha_{V\text{-}T}$. The Landau-Teller calculation predicts relaxation that is much slower than the experimental data. The SSH result provides somewhat better agreement with the data. Note also that the translational temperatures virtually overlay for the Landau-Teller and full solver calculations. The full master equation solver with SSH is able to predict the experimentally observed faster vibrational relaxation but satisfactory quantitative agreement is not achieved. Likely causes of this discrepancy are given in the next section. The computed population distribution for the full solver calculation is shown in Fig. 13. From this plot, we see that the vibrational temperature for the lowest levels freeze before $A/A^* = 2$ in the supersonic region. The middle and upper levels are very overpopulated and we see that population inversion occurs, i.e., the number density increases with quantum number.

Conclusions

It is shown, herein, that values for the interaction range parameter α can be inferred by comparing transition rates to experimental data. In particular, it is found that a value of $\alpha_{V\text{-}T} = 3.9\ A^{-1}$ for N_2 and $\alpha_{V\text{-}T} = 4.6\ A^{-1}$ for CO allow the temperature dependence of SSH V-T rates to match those rates found from Millikan and White experimental data. Values for the molecular constants needed in transition rate theories based upon other molecular models may also be inferred from a similar comparison method. There is significant uncertainty in V-V exchange transition rates computed from SSH theory. The effects of these V-V exchange rates are modeled by performing a parametric study of various V-V rates and by using various values of $\alpha_{V\text{-}V}$. It is found that higher values of $\alpha_{V\text{-}V}$ increase the effect of V-V exchange rates in accelerating vibrational relaxation in cooling flows. Through simulations of a cooling gas and a nozzle flow, it is found that vibrational relaxation is accelerated in conditions of high vibrational energy and low translational temperature. However, a parametric study of V-V exchange rates suggests that it is unlikely that these rates are solely responsible for the experimentally observed acceleration of vibrational relaxation in expanding flows. Overpopulation is seen in the middle and upper levels, and in the nozzle flow simulation population inversion is predicted. The acceleration mechanism found here agrees with that proposed by Treanor et al. and by Bray. The full master equation solver with SSH theory agrees qualitatively with experiments which predict faster relaxation than the Landau-Teller model but satisfactory quantitative agreement is not achieved. SSH transition rates will underpredict the overall relaxation rate only if there are very large errors in its scaling of the middle and upper levels relative to the ground state rates. Vibrational relaxation should be studied with alternate transition rate theories to determine if they can predict the experimentally observed rates. Also, as discussed in Ref. 2, the level of impurities in the experimental gas sample can have a significant effect on the measured relaxation rate. The effects of possible impurities in the experimental gas samples and radiative effects must be studied to determine the magnitude of the experimental arror and to resolve discrepancies in various experiments. Both of these issues must be addressed to allow quantitative agreement between computation and experiment.

References

[1]McLaren, T. I., and Appleton, J. P, "Vibrational Relaxation Measurements of Carbon Monoxide in a Shock Tube Expansion Wave," *Journal of Chemical Physics,* Vol. 53, No. 7, Oct. 1970, pp. 2850–2857.

[2]Hurle, I. R., "Nonequilibrium Flows with Special Reference to the Nozzle-Flow Problem," *Proceedings of the 8th International Shock Tube Symposium, Imperial College* (London), July 1971, pp. 3/1–3/37.

[3]Bray, K. N. C., "Vibrational Relaxation of Anharmonic Oscillator Molecules: Relaxation under Isothermal Conditions," *Journal of Physics B, Proceedings of Physics Society,* Vol. 1, No. 2, 1968, pp. 705–717.

[4]Treanor, C. E., Rich, J. W., and Rehm, R. G., "Vibrational Relaxation of Anharmonic Oscillators with Exchange-Dominated Collisions," *Journal of Chemical Physics,* Vol. 48, No. 4, Feb. 1968, pp. 1798–1807

[5]Blom, A. P., Bray, K. N. C., and Pratt, N. H., "Rapid Vibra-

tional De-excitation Influenced by Gasdynamic Coupling," Astronautica Acta, Vol. 15, No. 5/6, 1970, pp. 487–493.

[6]Schwartz, R. N., Slawsky, Z. I., and Herzfeld, K. F., "Calculation of Vibrational Relaxation Times in Gases," *Journal of Chemical Physics,* Vol. 20, No. 10, 1952, pp. 1591–1599.

[7]Clarke, J. F., and McChesney, *Dynamics of Relaxing Gases,* Butterworths Publishing, Reading, MA, 1976, Chap. 3.

[8]Sharma, S. P., Huo, W. M., and Park, C., "Rate Parameters for Coupled Vibration-Dissociation in a Generalized SSH Approximation," *Journal of Thermophysics and Heat Transfer,* Vol. 6, No. 1, 1992, pp. 9–21.

[9]Keck, J., and Carrier, G., "Diffusion Theory of Nonequilibrium Dissociation and Recombination," *Journal of Chemical Physics,* Vol. 43, No. 7, 1965, pp. 2284–2298.

[10]Billing, G. D., "Vibration-Vibration and Vibration-Translation Energy Transfer, Including Multiquantum Transitions in Atom-Diatom and Diatom-Diatom Collisions," *Nonequilibrium Vibrational Kinetics,* Topics in Current Physics, Vol. 39, Springer-Verlag, Berlin, 1986, pp. 85–112.

[11]Millikan, R. C., and White, D. R., "Systematics of Vibrational Relaxation," *Journal of Chemical Physics,* Vol. 39, No. 12, 1963, pp. 3209–3213.

[12]Hirschfelder, J. O, Curtiss, C. F., and Bird, R. B, *Molecular Theory of Gases and Liquids,* Wiley, New York, 1954, pp. 1110–1111.

[13]Landrum, D. B., and Candler, G. V., "Vibration-Dissociation Coupling in Nonequilibrium Flows," AIAA Paper 91-0446, Jan. 1991.

[14]Billing, G. D., and Fisher, E. R., "VV and VT Rate Coefficients in N_2 by a Quantum-Classical Model," *Journal of Chemical Physics,* Vol. 43, No. 3, 1979, pp. 395–401.

[15]Radzig, A. A., and Smirnov, B. M., *Reference Data on Atoms, Molecules, and Ions,* Springer Series in Chemical Physics, Vol. 31, Springer-Verlag, Berlin, 1985, p. 315.

[16]Landrum, D. B., private communication, North Carolina State Univ., Raleigh, NC, June 1991.

[17]Taylor, R. L., and Bitterman, S., "Survey of Vibrational Relaxation Data for Processes Important in the CO_2-N_2 Laser System," *Reviews of Modern Physics,* Vol. 41, No. 1, 1969, pp. 26–47.

[18]Sharma, R. D., and Brau, C. A., "Energy Transfer in Near-Resonant Molecular Collisions due to Long-Range Forces with Application to Transfer of Vibrational Energy from u_3 Mode of CO_2 to N_2," *Journal of Chemical Physics,* Vol. 50, No. 2, Jan. 1969, pp. 924–930.

[19]Lomax, H., "Stable Implicit and Explicit Numerical Methods for Integrating Quasi-Linear Differential Equations with Parasitic-Stiff and Parasitic-Saddle Eigenvalues," NASA TN D-4703, May 1968.

[20]Hall J. G., and Treanor, C. E., "Nonequilibrium Effects in Supersonic-Nozzle Flows," Cornell Aeronautical Lab., Rept. 163, Buffalo, NY, March 1968; also AGARDograph 124, Dec. 1967.

[21]von Rosenberg, C. W., Jr, Taylor, R. L., and Teare, J. D., "Vibrational Relaxation of CO in Nonequilibrium Nozzle Flow," *Journal of Chemical Physics,* Vol. 48, No. 12, 1968, pp. 5731–5733.

Ernest V. Zoby
Associate Editor